Received: 31 March 2020 | Accepted: 12 August 2020

DOI: 10.1111/mms.12745

ARTICLE

Marine Mammal Science

Assessing the lethality of ship strikes on whales using simple biophysical models

Dan E. Kelley[1] | James P. Vlasic[1] | Sean W. Brillant[1,2]

[1]Dalhousie University, Department of Oceanography, Halifax, Nova Scotia, Canada

[2]Canadian Wildlife Federation, Kanata, Ontario, Canada

Correspondence
Sean Brillant, Dalhousie University, Department of Oceanography, PO Box 15000, 1355 Oxford Street, Halifax, Nova Scotia B3H 4R2, Canada.
Email: seanb@cwf-fcf.org

Abstract

Studies of ship strikes on whales often focus on large vessels (>20 m), with attention to their speeds and the resulting risk of lethality. Smaller coastal vessels also co-occur with whales, resulting in collisions that merit study. To cast light on injuries caused by vessels of all sizes, we used knowledge of right whale anatomy and Newtonian mechanics to construct simple models that predict the mechanical stresses experienced by whales during collisions. By comparing our predictions with published models and with data from ship strikes on various whale species, we developed a model for lethal injury as a function of several vessel and whale properties, finding that collisions that create stresses in excess of 0.241 MPa were likely to cause lethal injuries to large whales. Furthermore, this model has revealed that (1) vessels of all sizes can yield stresses higher than this critical level, and (2) large vessels produce stresses much larger than this even when travelling at reduced speeds (i.e., 10 knots). The model is fast enough to power an interactive GUI-based tool (in R) and flexible enough to simulate strikes by vessels of different masses and speeds upon whales of different species, sizes, and physical conditions.

KEYWORDS

biophysical model, lethality, mechanical stress, North Atlantic right whale, policy, ship strikes, shipping, speed restrictions, whales

1 | INTRODUCTION

Collisions with whales by ocean-going vessels (i.e., ship strikes) have been widely studied (Conn & Silber, 2013; Gende et al., 2019; Kite-Powell, Knowlton, & Brown, 2007; Laist, Knowlton, Mead, Collet, & Podesta, 2001; Schoeman, Patterson-Abrolat, & Plön, 2020; van der Hoop, Vanderlaan, & Taggart, 2012; Vanderlaan, Taggart, Serdynska, Kenney, & Brown, 2008). The observations compiled by Laist et al. (2001) suggest that the most severe injuries occur as a result of ship strikes by large vessels, and accordingly both the United States and Canada have made efforts to mitigate this problem by altering traffic patterns and restricting the speeds of large vessels (length > 20 m; e.g., Transport Canada, 2018; U.S. Federal Register, 2008). There are, however, many smaller vessels (length < 20 m) that can also be involved in ship strikes, and some observations indicate that injuries from these collisions can be serious (Jensen & Silber, 2004; Neilson, Gabriele, Jensen, Jackson, & Straley, 2012; Ritter, 2012; Wiley, Mayo, Maloney, & Moore, 2016). These smaller vessels generally do not use automatic identification systems (AIS), thus producing less track-data compared to larger vessels and they are not subject to the regulations to mitigate ship strike lethality (Transport Canada, 2018). This suggests it is a mistake to focus solely on large vessels, particularly given recent observations of right whales in coastal eastern Canadian waters, where smaller vessels are used in local fisheries that are active at times while the whales are present (Davies & Brillant, 2019; Simard, Roy, Giard, & Aulanier, 2019).

It can be difficult to diagnose the trauma responsible for the death of whales killed by ship strikes without a forensic necropsy because external indicators of the injury may be few or subtle (Campbell-Malone et al., 2008). A further complication is that there is no single indicative condition that signifies mortality by blunt trauma. For example, necropsies of whales killed by blunt trauma typically report extensive subcutaneous hemorrhages that can extend through the blubber and the underlying tissues (Moore et al., 2013), but the occurrence of broken bones is neither universal, nor diagnostic. Campbell-Malone et al. (2008) report that the mandibles of North Atlantic right whales (*Eubalaena glacialis*; hereafter, right whales) were fractured in one-third of the necropsies they examined where blunt trauma was identified as cause of death. Sharp et al. (2019) reported that 8 of 10 right whales killed by blunt trauma had fractured bones. Similarly, three of the four right whales determined to have died as a result of blunt trauma in Canada in 2017 had acute internal hemorrhages, but, importantly, just one of these animals had bone fractures that were attributable to the blunt trauma that resulted in the death of the animal (Daoust, Couture, Wimmer, & Bourque, 2018). These observations indicate that the stresses experienced by whales during ship strikes do not need to exceed the breaking strength of bones to kill the animal.

Motivated by the desire to investigate the potential for serious injury by small vessels, and to reduce uncertainties in the mode of injury by vessels of all sizes, we set out to quantify the reactive forces that arise during ship strikes with large whales. By demonstrating the relationship between strikes and the reactive forces of the collision, our goals were to provide a more complete evaluation of the threat that vessels of all sizes pose to whales, and to identify the physical factors that influence this threat. Many species of whales are struck by vessels (Jensen & Silber, 2004; Neilson et al., 2012; van der Hoop et al., 2013) and so we set out to create models that could deal with whales and vessels of all sizes and types. The particular focus was, however, on right whales, which puts our work in the context of a growing body of knowledge about right whale ship strikes, the biophysical studies of right whales (e.g., Raymond, 2007), and the relationship of vessel speeds and lethality (e.g., Conn & Silber, 2013; Vanderlaan & Taggart, 2009).

2 | METHODS

2.1 | Model formulation

2.1.1 | One-layer scaling model

The main tool used in the present study is a four-layer model that will be described in the next section. However, we begin by describing a simpler model, to establish the notation and to cast some light on the basic dynamical

principles. This system involves the collision of a large object of mass M_s moving at velocity V_s until it collides with a much lighter stationary object of mass M_w. Here, the subscripts *s* and *w* stand for ship and whale, respectively. Supposing both ship and whale to be point masses separated by a compressible layer of thickness *l* that has linear elastic modulus of compression *E*, the force resisting collision may be written $F = AE\Delta l/l$, where *A* is the impact area and Δl measures the compaction at any given time. Denoting positions of the ship and whale as X_s and X_w, and setting $t = 0$ as the time of initial contact of the ship with the compressible layer, we may write $\Delta l = l - (X_w - X_s)$, during the interaction interval. According to Newton's second law, the momentum equations for ship and whale are

$$M_s \frac{dV_s}{dt} = -F \tag{1}$$

and

$$M_w \frac{dV_w}{dt} = F \tag{2}$$

where ship and whale velocities are $V_s = dX_s/dt$ and $V_w = dX_w/dt$, respectively, and a positive value of *F* indicates a force in the direction of increasing *x* coordinate. For the case of a large ship and a much smaller whale, we have $M_s \gg M_w$, so that combining Equations 1 and 2 reveals that $\left|\frac{dV_s}{dt}\right| \ll \left|\frac{dV_w}{dt}\right|$. This means that the ship is too massive to be slowed appreciably during the collision. In this limit, Δl may be approximated as $l + Vt - X_w$ where *V* denotes the nearly constant ship speed. Thus, the whale's momentum equation can be written

$$\frac{d^2X_w}{dt^2} = \frac{AE}{M_w}\left(\frac{l + Vt - X_w}{l}\right) \tag{3}$$

It is convenient to define a new variable $\zeta = X_w - l - Vt$, which is the negative of Δl in this limiting case of a constant-velocity ship. With this definition, Equation 3 becomes

$$\frac{d^2\zeta}{dt^2} + \omega^2\zeta = 0 \tag{4}$$

where $\omega = \sqrt{AE/(lM_w)}$. This is an oscillation equation, with solution

$$\zeta \propto \sin \omega t \tag{5}$$

given the initial condition $\zeta = 0$ at $t = 0$. The absolute value of this function reaches a local maximum when $\omega t = \frac{\pi}{2}$ so a time scale for the penetration of the ship into the body of the whale is

$$t_* = \frac{\pi}{2}\sqrt{\frac{lM_w}{AE}} \tag{6}$$

Thus, ignoring whale movement to first order, so that $d\zeta/dt = 0$ at $t = 0$ can be approximated as $-V$, we may derive

$$\zeta_* = V\sqrt{\frac{lM_w}{AE}} \tag{7}$$

as a length scale for the penetration of the ship into the body of the whale.

Although limited by approximations that will be relaxed in the next section, these simple formulas may still be useful for building intuition. As might have been expected, both the impact time, t^*, and the depth of penetration, ζ^*, are predicted to increase with whale length, since larger whales have larger mass and also thicker regions of blubber and other compressible materials. However, and perhaps not so intuitively, the square root implies that neither of these dependencies is linear. The square root dependence also applies, inversely, to the relationship of impact time and penetration to the area of impact, A, and the stiffness of the compressible material, E. Thus, the formulas back up and extend the intuition that a sharply pointed ship prow will penetrate further than a blunt one, and that penetration will be deeper for more compressible material.

More insight on the penetration depth can be gathered by focussing on ζ^*/l, the fractional compaction of the compressible layer. It might be hypothesized that high values of this quantity may correlate with high potential for injury. It is instructive to write this as

$$\frac{\zeta^*}{l} = \frac{V}{V_0} \tag{8}$$

whereupon

$$V_0 = \sqrt{\frac{AEl}{M_w}} \tag{9}$$

may be interpreted as a scale for critical ship speed, as it corresponds with complete tissue compaction. With reasonable values (explained and refined below) $A = 1.32\ \text{m}^2$, $E = 0.6 \times 10^6$ Pa (section 2.2.5 in Raymond, 2007), $l = 1.3$ m (sum of thickness of skin, blubber, and sublayer) and $M_w = 20 \times 10^3$ kg, we find that $V_0 = 7.2$ m/s (or 14 knots). This speed is comparable to the Vanderlaan & Taggart (2007) estimate of a critical speed of 6.1 m/s (or 11.8 knots) for increased likelihood of lethality of large-ship impacts. Even so, the assumptions underneath this calculation are so crude that the results should be considered mostly as a scaling relationship that provides context for a more realistic model. The next section provides such a model, in which the dynamical approximations are less restrictive, and the biomechanical model of whale tissue is more realistic.

2.1.2 | Four-layer model

A simple way to extend the previous model is to replace its single layer of compressive material with a sequence of layers that have distinct thicknesses and material properties. Our tests with a variety of configurations revealed that a simple but reasonable arrangement is to consider four such layers: a skin layer, a blubber layer to its interior, a region further to the interior that we will call the sublayer, and bone to the interior of that. The literature provides direct or indirect guidance as to the material properties of each of these layers except the sublayer, and so in this treatment we will follow Raymond (2007) in taking the sublayer material properties to be similar to those of the blubber, although the model is constructed to permit distinct sublayer properties.

The notation already established for ship and whale mass, position, velocity and acceleration will be retained in this model. The forces considered during the impact event are the resistance of the whale's body to compression (although now in four layers), the resistance of the whale's skin to extension across the deformed impact zone, water drag on both ship and whale, and the ship's thrust. Importantly, (1) no assumptions are made on the ratio of whale acceleration to ship acceleration, so the model will handle a range of ship masses and (2) the assumption of a linear stress–strain relationship is dropped, to improve the accuracy of force calculations.

In the interests of simplicity of this initial study, only normal (i.e., not oblique) impacts are considered, and the shearing effects of propeller blades on skin are ignored. Ship deformation is ignored on the assumption that it will be

negligible compared to deformation of the whale. That deformation is assumed to be confined to a particular impact area that is modelled as rectangular, while retaining the ability to address actual prow shapes by geometric calculations. For the present purpose, the key material property of the constituent whale layers is the stress–strain relationship. (The model also tracks material strength, but this is mainly for future work as, at present, the literature provides few constraints on this property.) Water drag forces are expressed in a standard quadratic form that involves the wetted areas of the vessel and whale, and the square of the speeds of each with respect to the surrounding water, which is assumed to be motionless relative to an assumed nonaccelerating coordinate system.

With these assumptions, the dynamical system may be expressed as a small set of algebraic and ordinary differential equations.

Prior to contact, the ship momentum equation is expressed as

$$M_s \frac{dV_s}{dt} = T_s - D_s \tag{10}$$

where T_s is the ship thrust (i.e., propulsive force) and D_s, the drag force, is parameterized with

$$D_s = -\frac{1}{2}\rho S_s C_s V_s |V_s| \tag{11}$$

where ρ is water density, S_s is the vessel's wetted surface area, and C_s is a nondimensional factor that accounts for frictional and other forms of drag on the ship (van Manen & van Oossanen, 1988). The default value of C_s is taken to be four times the purely frictional value of $CF = 2.5 \times 10^{-3}$ given in fig. 4 of van Manen & van Oossanen (1988), for the Reynolds Number appropriate to fishing boats moving at 10 knots, on the assumption that friction typically accounts for about a quarter of the total drag on low-speed vessels (MAN Diesel & Turbo, 2011). As a test, the drag force as formulated was used to predict the power consumption of a typical Cape Islander fishing boat, using reasonable values for engine and propeller efficiency. The results matched to within a factor of 2, and since this is comparable with the variation in hull resistance caused by biofouling through the course of a season (Woods Hole Oceanographic Institution, 1952), this was taken as confirmation of the acceptability of the drag formulation.

During contact, we must account for forces resulting from deformation of the whale. Denoting the sum of such forces as F (with positive values meaning that the whale will be accelerated in the X direction), Equation 10 may be extended to

$$M_s \frac{dV_s}{dt} = T_s - D_s - F. \tag{12}$$

The model takes the ship thrust T_s to be a constant value implied by the thrust-friction balance for the velocity prior to the collision, on the assumption that the vessel operator will be unable to cut engine power in the subsecond timescale of a collision. However, the drag force D_s is taken to vary with ship speed according to the quadratic drag law discussed above.

On the assumption that an initially motionless whale will not be able to respond during the brief interval of a collision event, its swimming thrust T_w can be set to zero, yielding the momentum equation

$$M_w \frac{dV_w}{dt} = F - D_w \tag{13}$$

where D_w, which accounts for water drag, is formulated with a quadratic law similar to that of the ship, but with drag coefficient C_w of 2.5×10^{-3}, on the assumption that the whale drag will not involve the

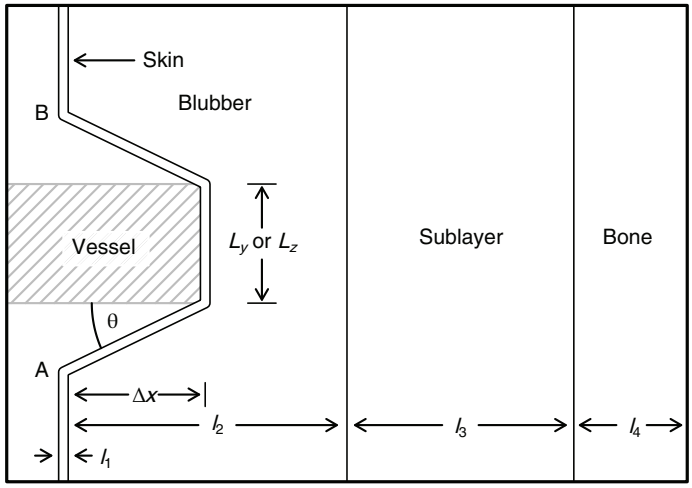

FIGURE 1 Definition sketch (not to scale) showing the cross-sectional geometry of four-layer model of a whale being impacted by a moving vessel.

wave-making and form-drag components that apply to ships moving under power. Sensitivity experiments with the model (Appendix A), suggest that the overall results depend very little on the details of the drag parameterizations, simply because these forces are very small (by factors exceeding 100), compared with the impact forces.

The reactive force, F, is broken down into two components, viz.

$$F = F_C + F_E \tag{14}$$

where F_C is a compression force resulting from the thinning of whale skin, blubber, sublayer, and bone, and F_E is an extension force resulting from the stretching of skin over the depression made by the ship as it protrudes into the animal. Figure 1 illustrates the geometry of the deformation, and also details some further notation about whale properties.

The core of the model formulation lies in the expression of F_C and F_E in terms of the penetration of the ship into the whale. The compression force is perhaps the most straightforward, so it will be discussed first. A nonlinear stress–strain relationship is assumed for the compression of skin, blubber, sublayer, and bone. In this, the engineering stress σ (i.e., the normal force per unit area) is related to the engineering strain (i.e., the fractional reduction in thickness) with

$$\sigma_i = a_i\left(e^{b_i\epsilon} - 1\right) \tag{15}$$

where subscript i is 1 for skin, 2 for blubber, 3 for sublayer, and 4 for bone. The exponential form of this proposed relationship is consistent with the approximately linear dependence of local modulus (i.e., $\partial\sigma/\partial\epsilon$) on stress σ for Cuvier's beaked whale (*Ziphius cavirostris*), shown in fig. 8 of Soldevilla *et al*. (2005). Furthermore, this form works well as a regression model for the stress–strain relationship shown in fig. 2.13 of Raymond (2007). Some insight on this formulation is gained by noting that the b_i values indicate the nonlinearity of the stress–strain relationship in each layer, and that the product a_ib_i approaches the linear modulus E_i in the limit of low strain, since $e^{b_i\epsilon} \approx 1 + b_i\epsilon$ for small values of $|b_i\epsilon|$.

The key variable in the formulation of the reactive force is the penetration Δx of the ship into the whale (again, see Figure 1). Denoting the strains within the individual layers ε_1 through ε_4, we may write this penetration distance as

$$\Delta x = \sum_i \epsilon_i l_i \tag{16}$$

Limiting the sum to just those layers that have nonzero thickness (i.e., to layers that have compression strain $\varepsilon_i < 1$) enables the model to handle cases of fast vessels or strikes on parts of the whale that have little cushioning between skin and bone.

Combining Equations 15 and 16 yields

$$\Delta x = \sum_i (l_i/b_i)(1 + \ln(\sigma/a_i)) \tag{17}$$

as the key link between force and vessel-whale separation. The meaning of this equation is revealed by considering the case of σ and a_i of the same order, because then $\ln(\sigma/a_i) \approx (\sigma/a_i - 1)$, so that the right-hand side of Equation 17 becomes $\sigma\sum_i l_i/a_i b_i$. With a linear approximation to the stress–strain relationship, this becomes $\sigma\sum_i l_i/E_i$, revealing that layers that are much thinner than others can be neglected, as can layers that are much stiffer than others. This applies to both skin and bone, and so the thickness and the stiffness of these components do not affect the compression force F_C greatly, provided that the intermediate layers have been compressed only slightly. However, this assumption of slight compression fails during a strong collision, during which bone compression can suddenly yield large forces that greatly overwhelm the forces created by the compression of the softer materials during the earlier stages of the impact. (This sudden force is analogous to the jolt that may be felt when an automobile's suspension spring bottoms out over a large bump in the road.)

As an aside on computational aspects, it is worth pointing out that Equation 17 is not easily inverted, and so it is solved in the model by using a root-finding method. Since this is a computationally expensive calculation that would be needed at every time-step in the simulation, the model computes the $\sigma = \sigma(\Delta x)$ relationship just once, at the start of the simulation, caching the results in a piecewise-linear approximating function that can be computed quickly as the simulation proceeds.

Returning to the dynamics of ship and whale, the compression force is found by multiplying stress σ by the impact area, which in the model is the product of a horizontal extent L_y and a vertical extent L_z (again, see Figure 1), i.e.,

$$F_C = L_y L_z \sigma \tag{18}$$

This leaves a single force to be discussed, namely that resulting from the extension of skin over the dimpled region of impact. There is little guidance in the literature for formulating this force, so a simple model is constructed here. The area of direct contact is assumed to be surrounded by a linearly beveled region that makes angle θ to the direction normal to the skin surface. The stretching is assumed to be constant throughout the depressed region (including the bevel), i.e., the skin that originally extended along a line from A to B in the definition sketch of Figure 1 becomes stretched from its original length along a line connecting the points to the longer path indicated by the three line elements on the diagram. The strain in the *y*-direction can therefore be written

$$\epsilon_y = 2\frac{\Lambda - \lambda}{L_y + 2\lambda} \tag{19}$$

where $\Lambda = \Delta x/\cos\theta$ and $\lambda = \Delta x \cdot \tan\theta$, after which an analog to Equation 15 can be used to compute along-layer tensile stress σ_y in the y-direction. Analogous steps lead to σ_z for skin stress in the z-direction. Multiplying these stresses by the nominal skin thickness l_1 along the perimeter of the impact zone, and then by the lengths of the corresponding sides, yields net force

$$F_E = 2l_1(L_y\sigma_z + L_z\sigma_y)\cos\theta \quad (20)$$

in the x-direction, with forces in the y- and z-directions cancelling by symmetry.

Taken together, Equations 10 to 20 form the basis of the four-layer numerical model that is the centerpiece of the present study. The integrations of the differential equations are carried out with the "lsoda" function in the R language (R Core Team, 2020), which is supplied as part of the "deSolve" package for numerical integration of differential equations (Soetaert, Petzoldt, & Setzer, 2010). This function is well-suited to the present application because of its high accuracy in mathematically stiff problems, i.e., problems with rapidly changing temporal behaviors, as can occur with a bone compression, as explained above. Appendix B explains how the simulation code is made available to readers as an R package named "whalestrike" and Appendix C explains the choice of default values for a_i, b, θ, etc., used in that package, and in most of the following.

2.2 | Comparison with Raymond's (2007) simulations

The model was configured to represent a mid-body strike of a 13.7 m North Atlantic right whale weighing 30 tonnes (i.e., 30,000 kg; Fortune et al., 2012), and the thicknesses of the layers l_1 through l_4 (i.e., skin, blubber, sublayer, and bone) set to 0.025 m, 0.16 m, 1.12 m, and 0.1 m respectively. These values were selected to match the values used by Raymond (2007), and the thicknesses of the layers reasonably match values measured during necropsies of adult right whales (Daoust et al., 2018; Leighfield, 2003).

The simulations used a ship of mass 311 tonnes with a bulb at the bow, as detailed in the finite-element calculations of Raymond (2007). Examination of Raymond's diagrams of whale deformation, together with calculations of the geometry of intersecting shapes, suggests representing the ship's bulb-shaped impact zone with L_y = 1.24 m and L_z = 0.71 m in the present framework. As in Raymond (2007), it was assumed that the biomechanical properties of the sublayer matched those of the blubber layer. The sublayer thickness was increased from the default model value of l_3 = 1.12 m to 1.47 m, to account for the unexpectedly high mass of the Raymond (2007) simulated whale, which Raymond (and the present authors) took to indicate an error in inferred girth. The default values were used for the other layers of the model whale.

2.3 | Estimating the lethality of the reactive forces of a whale strike

We examined published historical records of observed whale strikes for which we could determine (or reasonably assume) the variables needed to set up collision simulations with the four-layer model (i.e., vessel size, vessel speed, whale size, fate of the whale; Table 1). We limited our analysis to those observations where the fate of the whale was recorded as "no injury," "minor injury," "serious injury," or "killed." Some observations of whales that have been struck by ships report that the animal was swimming or acting "normally" following the ship strike (Laist et al., 2001), but there are also many observations to support the notion that animals may ultimately die as a result of earlier injuries (Campbell-Malone et al., 2008; Kraus et al., 2005; Moore et al., 2013; Neilson et al., 2012; Sharp et al., 2019). Lacking definitive results in the literature, we chose to simplify matters, categorizing reports of both "no injury" and "minor injuries" as nonlethal outcomes and both "serious injuries" and "killed" as lethal outcomes, in the same manner as previous studies (Conn & Silber, 2013; Neilson et al., 2012; Vanderlaan & Taggart, 2007). In total, we uncovered 34 observations that had the information required for comparison with model simulations. For each observation, the four-layer model was used to estimate the maximal reactive forces during collision, and these results were linked to the fate of the whale (i.e., nonlethal or lethal). The resulting relationship was used to infer a function linking the inferred probability of lethality, P(lethal), to the modeled collision stresses on the whale. Since those stresses are controlled by ship speed, mass, and contact area, along with whale biomechanical properties, the result of a successful linkage will be a tool that may be used to predict the outcomes of arbitrary whale strikes.

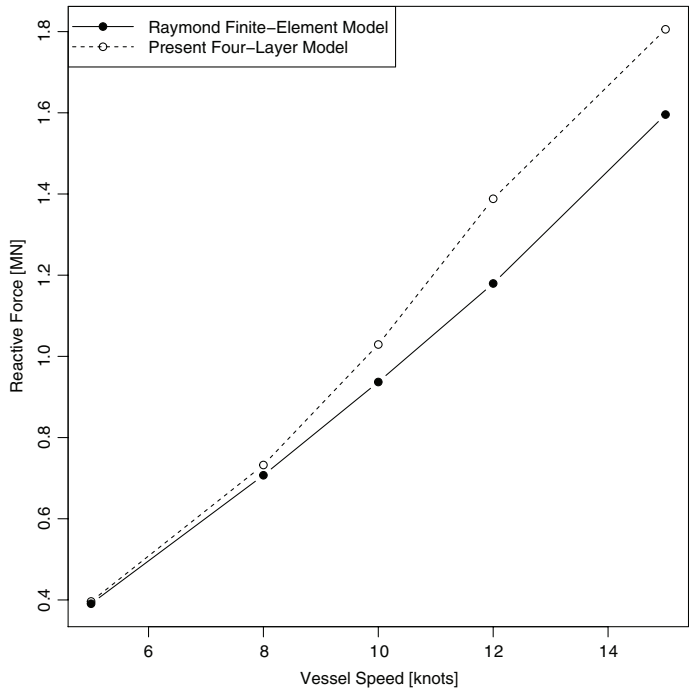

FIGURE 2 Comparison of the predicted dependence of collision stress (force per unit area) for impacts by a 311-tonne ship moving at selected speeds. The solid curve represents the results of the finite-element simulations of Raymond (2007) as reported in his Figure 6.1, and the dashed curve represents the results of the present four-layer simulation, showing the sum of compression and extension forces.

3 | RESULTS

Before moving on to the main results of the analysis, it should be noted that comparisons of the predictions between the four-layer model and the one-layer model were done throughout the analysis. This comparison relied on the fact that these simulations assumed equal biomechanical properties for blubber and sublayer, so computation of the equivalent thickness in a one-layer model was direct. As expected, the model predictions diverged most for the simulations involving a small vessel, for which it is unreasonable to assume that the vessel will maintain constant speed during a collision. The differences in predictions are significant in practical terms. For example, critical speeds for a 45-tonne boat (discussed later) differ by up to 26% between the one-layer and the four-layer models, and by 9% for a 311-tonne ship. Since a prime motivation for the present work was to study collisions with small vessels, and since we hope to establish a foundation for further studies with distinct biomechanical properties in each layer, we will focus entirely on the four-layer model in the remainder of this paper.

3.1 | Comparison with Raymond (2007)

Raymond (2007) produced a summary diagram (his fig. 6.1) showing maximum compression stress within the whale, as a function of ship speed, and this provides a convenient way to test the present model. Overall, the root-mean-square difference between the stress predictions of the finite-element and four-layer models was 0.14 MN, or 9.4% of the signal, with the results being nearly identical at low speeds (Figure 2). Since no "tuning" had been done by adjusting material properties to match the models, this agreement serves as a practical validation of the four-layer model.

TABLE 1 Reported ship strikes used to produce the lethality curve, where L (m) is length in meters, and Wt (t) is mass in tonnes. Fate is a description of the reported state of the whale after the ship strike; Uninjured and Killed are self-explanatory, and Minor and Serious each refer to the reported severity of the injury to the whale. Type is the reported description of the vessel where "HS Ferry" is a high-speed ferry, "USCG" is a US Coast Guard vessel, and "WW" is a whale watching vessel. Sp (kn) is the reported speed in knots of the vessel when the strike occurred. Max. stress is the maximum value of stress in megapascals computed during a numerical simulation with the four-layer model, based on the other properties listed in this table.

		Whale				Vessel					
Case	Date	Species	L (m)	Wt (t)[a]	Fate	Type	L (m)	Wt (t)[b]	Sp (kn)	Max. stress (MPa)	Reference
1	1885-01-01	Large whale	—	40	Minor	Pilot	—	60	13	0.92	Laist et al. 2001
2	1935-01-01	Large whale	—	40	Killed	Steamship	131	30,000	15	114.24	Laist et al. 2001
3	1953-11-01	Large whale	—	40	Killed	Navy	169	11,100	20	819.23	Laist et al. 2001
4	1955-03-22	Sperm whale	14	29	Killed	Steamship	144	30,000	17	1.78	Laist et al. 2001
5	1961-09-01	Large whale	—	40	Serious	Cargo	—	8,000	14	1.67	Laist et al. 2001
6	1972-12-01	Right whale	13	26	Killed	Container	207	24,182	22	647.77	Laist et al. 2001
7	1974-04-23	Large whale	—	40	Serious	Yacht	18	15	10.5	0.34	Laist et al. 2001
8	1974-12-01	Large whale	—	40	Serious	Ferry	—	4,000	17	540.24	Laist et al. 2001
9	1975-01-22	Gray whale	14	31	Killed	Navy	—	72	51	822.51	Laist et al. 2001
10	1980-07-05	Blue whale	30	183	Killed	Tanker	203	80,000	21	824.46	Laist et al. 2001
11	1984-08-01	Fin whale	24	80	Serious	WW	28	70	16	289.14	Laist et al. 2001
12	1988-09-07	Right whale	13	26	Killed	Ferry	171	8,000	12.5	0.92	Laist et al. 2001
13	1991-06-21	Humpback whale	15	49	Minor	WW	14	60	7.5	0.40	Laist et al. 2001
14	1991-07-06	Right whale	4.6	1	Killed	USCG	84	3,500	22	0.17	Laist et al. 2001
15	1992-02-01	Sperm whale	14	29	Killed	HS Ferry	20	5	45	17.88	Laist et al. 2001
16	1992-04-04	Large whale	—	40	Serious	Research	89	3,500	14	1.66	Laist et al. 2001
17	1992-05-15	Bryde's whale	12	12	Killed	Container	121	50,000	14	0.58	Laist et al. 2001
18	1993-09-09	Fin whale	24	80	Killed	Ferry	159	40,000	20	820.53	Laist et al. 2001
19	1995-06-01	Large whale	—	40	Minor	Fishing	27	60	9	0.49	Laist et al. 2001
20	1996-01-16	Humpback whale	15	49	Uninjured	WW	25	10	9	0.22	Jensen & Silber 2004
21	1996-05-16	Large whale	—	40	Serious	USCG	115	3,300	15	47.32	Laist et al. 2001
22	1997-01-01	Sperm whale	14	29	Killed	Ferry	100	11,000	25	819.40	Laist et al. 2001

TABLE 1 (Continued)

Case	Date	Whale				Vessel				Max. stress (MPa)	Reference
		Species	L (m)	Wt (t)[a]	Fate	Type	L (m)	Wt (t)[b]	Sp (kn)		
23	1997-10-12	Sperm whale	14	29	Uninjured	Fishing	—	30	6	0.18	Jensen & Silber 2004
24	1998-04-24	Gray whale	9	7	Killed	Navy	172.8	9,800	14	0.37	Jensen & Silber 2004
25	1998-04-28	Gray whale	6	2	Killed	Navy	153.9	9,800	22	0.28	Jensen & Silber 2004
26	1998-08-01	Minke whale	11	13	Killed	HS Ferry	36	3,500	25	1.73	Laist et al. 2001
27	1998-08-11	Humpback whale	15	49	Uninjured	WW	23.8	10	2	0.03	Jensen & Silber 2004
28	1998-09-12	Minke whale	6	3	Killed	WW	24	65	25	0.46	Laist et al. 2001
29	1999-07-28	Humpback whale	12	25	Killed	Cruise	243.8	50,000	19	130.12	Laist et al. 2001
30	2000-01-11	Bryde's whale	12.4	13	Killed	Cruise	214	50,000	22	1.37	Laist et al. 2001
31	2000-02-01	Humpback whale	15	49	Serious	Passenger	118	14,000	14.3	355.08	Laist et al. 2001
32	2001-02-26	Humpback whale	15	49	Uninjured	Inflatable	5.8	2	14	0.14	Jensen & Silber 2004
33	2001-06-18	Sperm whale	14	29	Killed	Navy	154	8,000	27	819.64	Jensen & Silber 2004
34	2001-06-29	Minke whale	7.6	5	Killed	Navy	253	10,000	15	0.32	Jensen & Silber 2004

[a]Masses for the whales were estimated to the nearest tonne based on their lengths using the equations from Fortune et al. (2012) for North Atlantic right whales and Lockyer (1976) for all other species. Where the length of the whale was not reported, we used the lengths for each species reported by NOAA (https://www.fisheries.noaa.gov/whales), rounded to the nearest meter. Where they report a range of lengths, we used the average, and where they reported a maximum length, we used the maximum length less 3 m. Where a ship strike record only reported "Large whale," we used 40 tonnes for its mass.

[b]Masses for vessels (i.e., displacement, not tonnage) were determined either by online searches for the named vessel, or by assuming the mass based on displacements of known vessels of the same type and length.

3.2 | Critical stress during ship strikes

A regression model of logistic form

$$P(\text{lethal}) = \left[1 + \exp\left(-\frac{\log_{10}\tau - c_1}{c_2}\right)\right]^{-1} \quad (21)$$

was chosen to represent the dependence of probability of lethality on the base-10 logarithm of compression stress (Figure 3, Table 1). Here, c_1 is the value of $\log_{10}\tau$ that yields P(lethal) = 0.5, and c_2 relates to the slope of the curve at the midpoint of the curve. A nonlinear least-squares method was used to infer c_1 and c_2, using the "nls" function in the R language, with related functions being used to calculate statistical characteristics of the fit. The resultant inferred value for c_1 was 5.38, SE = 0.15, p < .001, 95% CI [4.83, 5.65] while that for c_2 was 0.349, SE = 0.179, p = .061, 95% CI [0.123, 1.064]. The residual standard error of the regression was 0.326 with 32 df. Thus, the stress τ_{50} experienced by a whale during a ship strike that yields P(lethal) = .5 was estimated to be 0.241 MPa, 95% CI [0.067, 0.450].

The relationship between vessel speed and the modeled reactive stresses as a result of the ship strike are shown in Figure 4 for three different vessels. The masses (i.e., displacement, not tonnage) of the vessels were 45, 311, and 30,000 tonnes, representing plausible values for a typical coastal fishing boat in Atlantic Canada, a "large" vessel of the same mass used by Raymond (2007), and a still larger, more typical, container ship. The bow of the model coastal fishing vessel was patterned on the Cape Islander style that is typically used in Atlantic Canada, while the large vessels were modeled to have bulbs at their bow, as for the ship modeled by Raymond (2007). Accordingly, the areas of impact were set to 1.32, 0.88, and 0.88 m^2 for the three vessel types, respectively. The default values for whale biomechanical properties were used in the simulations, representing a mid-body strike of an adult right whale.

The resultant velocity that led to P(lethal) = .5 was 6.6 knots for the modeled 45-tonne fishing boat, 4.7 knots for the 311-tonne ship, and 4.5 knots for the 30,000-tonne ship. At 10 knots, the estimates of P(lethal) for a mid-body collision with a right whale were 0.69, 0.83, and 0.85 for these three vessel types. The simulations at 10 knots reveal that the whale would experience <5 g of acceleration during strikes by any of these vessels. These 10-knot simulations also indicate that the compressive forces on the bones are below the bone-breaking threshold, at least for mid-body strikes, where soft tissues are relatively thick.

The issue of the location of a ship strike along the body of the whale was addressed by calculating and plotting the critical velocity for various thicknesses of blubber and sublayer (Figure 5). The thickness of the blubber and

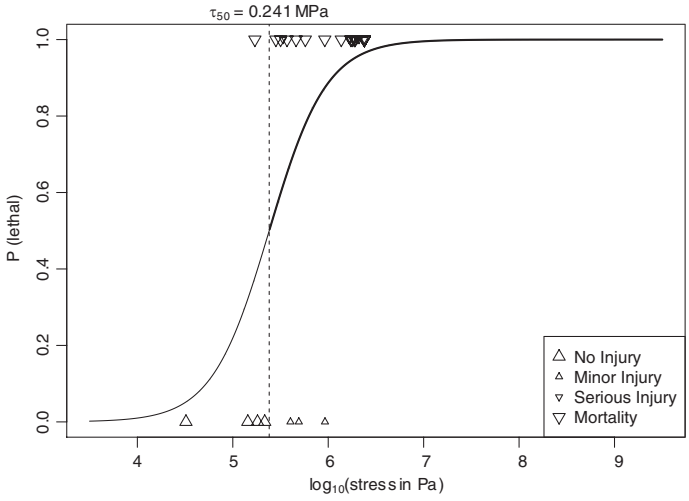

FIGURE 3 Probability of a lethal injury to a large whale in relation to the maximum compression stress incurred during a ship strike. The triangles represent literature results of ship strikes, with lethality characteristics as explained in the text, and with stresses inferred with model simulations that used the published ship and whale conditions. These points were fitted to a logistic function (solid line) to infer the probability of lethality, denoted P(lethal) in the text. The vertical dashed line indicates the stress, τ_{50}, that corresponds to the inflection of the logistic, i.e., the stress at which P(lethal) = .5, or the probability of lethality is 50%.

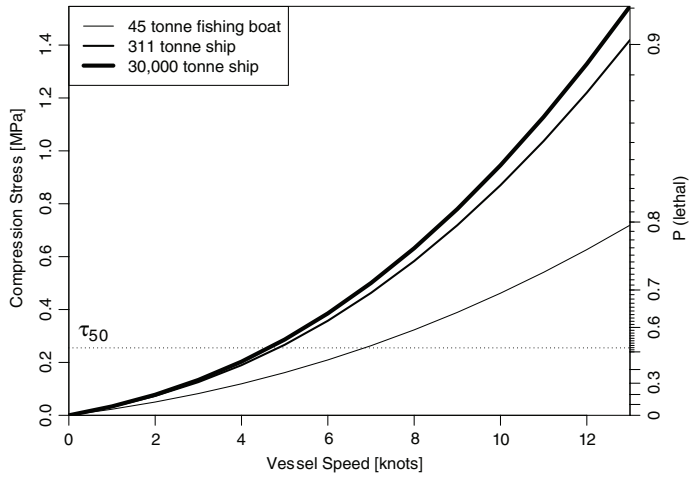

FIGURE 4 Variation of maximum compression stress with ship speed according to the four-layer model, for vessels of mass 45, 311, and 30,000 tonnes. The impact area for the 45-tonne fishing boat was set to 1.32 m^2, while for the larger ships, with protruding bulbous bows, it was set to 0.88 m^2. Default values are used for all other parameters. The horizontal line shows τ_{50}, the stress yielding a 50% probability of lethality.

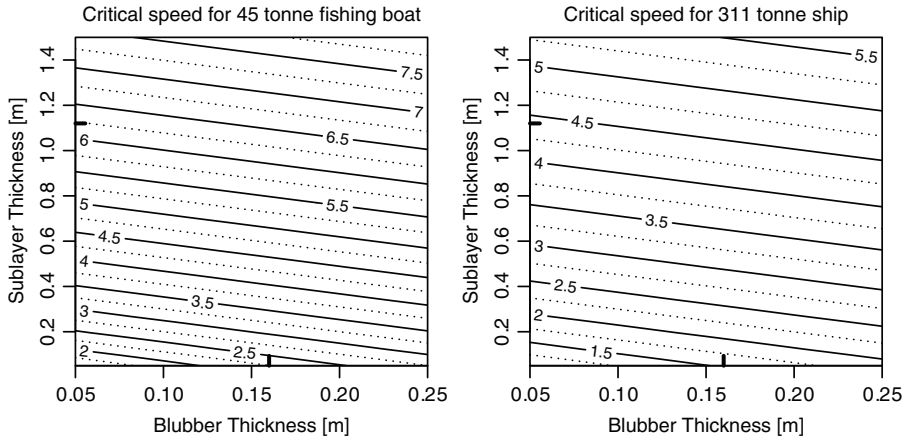

FIGURE 5 Dependence of the critical vessel speed, in knots, on the thickness of blubber and sublayer, for a 45-tonne fishing boat with impact area 1.32 m^2 (left) and a 311-tonne ship with impact area 0.88 m^2 (right). The contours show the collision speed that yields a compression stress that corresponds with *P*(lethal) = .5. The tick marks inside the axes show the default layer thickness values of the model, which are intended to represent a mid-body ship strike of a right whale. The velocities at the intersections of these tick marks match those at stress τ_{50} in Figure 4.

sublayer vary predictably along the length of the animal, with larger thicknesses corresponding to strikes nearer the middle of the body (the top right area of each plot panel in Figure 5) and smaller thicknesses corresponding to strikes in areas with thinner tissue layers over the bone, such as the head or mandible (lower left area of each plot in Figure 5). For each of the vessels modeled in these plots (45-tonne and 311-tonne), critical velocities were higher in areas where these layers were thicker and lower where blubber and sublayer were thin.

4 | DISCUSSION

The good agreement between the predictions of the four-layer model and the finite-element model of Raymond (2007) is of high practical significance, given the difficulty of setting up finite-element models and the simplicity of setting up (and extending) models such as those presented here.

An observational comparison of our models with the statistical studies of Vanderlaan & Taggart (2007) and Conn & Silber (2013) is also warranted. Both studies used a form of logistic function to model whale lethality as a function of vessel speed, and although there is overlap with the predictions of the four-layer model and these previous studies, the detailed results of the present study differ in several important ways. First, estimates in the present study for *P*(lethal) of a ship strike at 10 knots by small (45 tonne) and large (>300 tonne) vessels were each much larger (0.69 and > 0.83 respectively) than the estimate of >0.32 for vessels of all sizes by Vanderlaan & Taggart (2007) and approximately 0.57 by Conn & Silber (2013; based on their fig. 3). Second, our estimates of critical velocities, which yield *P*(lethal) = .5, were 6.6 knots and 4.5–4.7 knots for small (45 tonne) and large (>300 tonne) vessels respectively, while Vanderlaan & Taggart (2007) estimated the critical velocity for vessels of all sizes was 11.8 knots (95% confidence interval approximately 6.5 to 14 knots), and fig. 3 of Conn & Silber (2013) suggests a critical velocity of 9 knots, with a credible interval of approximately 2.6 knots to 11.4 knots.

Several factors may account for the differences between the predicted lethalities and critical speeds of the present study with those of previous studies. To begin with, these are very different analyses, ours being based on Newtonian dynamics and biomechanical properties of whale tissue, and these other studies taking a more statistical approach. These previous studies modelled whale lethality only as a function of vessel speed, while the present study modeled whale lethality as a function of the mechanical stresses of the strikes, incorporating several other factors absent from previous studies such as vessel mass, impact area, and whale biomechanical properties. There were also differences in data selection; our model required more details from the data (e.g., vessel and whale masses) and so the available data set was winnowed compared to these other studies, though all studies examining the lethality of ship strikes on whales, including the present study, are limited by relatively few observations of adequate information. The models of the present study were based on physical laws and biomechanical information from all sources known to us, and were constructed with an eye to future data and dynamical refinements. The goal was not just to advance our knowledge of the mode and consequences of injury to whales as a result of ship strikes, but also to create a framework that can be further elaborated in future investigations.

An important result of the present study, especially in the context of whales migrating between regions with different shipping traffic, is that whales can be seriously (i.e., lethally) injured as a result of collisions by vessels of a wide range of sizes. Intuition and simple theory both suggest that the precise value of ship mass may become unimportant for sufficiently large ships (because the ship will not slow down greatly during collision with a much less massive whale), and the four-layer model simulations verify this, revealing little dependence of compression stress on ship mass, once the latter exceeds a few hundred tonnes (Figure 4). Serious injury is, therefore, not a surprising result for strikes by large vessels, which can be orders of magnitude more massive than a whale. Even small fishing vessels (e.g., 45-ft Cape Islanders) have sufficient mass (approximating or exceeding the mass of even large whales) to lethally injure whales if they strike them, despite their typically slower speeds relatively to large cargo vessels. This is particularly likely for strikes on whales where the tissue layers are thin (Figure 5).

The simulations also shed light on the mode of injury. For example, although the inferred probability of lethality from mid-body strikes by large vessels at typical transiting velocities (e.g., 16–24 knots; Hatch et al., 2008; Wiley, Thompson, Pace, & Levenson, 2011) exceeds 0.9 and approaches 1, these simulations do not routinely involve compression stresses that are comparable to bone strength. The same was found with midbody strikes by small vessels at typical transiting velocities (e.g., 10.7 knots; Wiley et al., 2011). As a result, our simulations are in line with reports that not all whales killed by blunt trauma have fractured bones (Campbell-Malone et al., 2008; Sharp et al., 2019). The precise nature of such injuries deserves further study of whale biology. For example, it may be that strikes that yield relatively small stresses in the dorsal region may still cause lethal hemorrhages within the extensive vascular system that exists in the layers below the blubber in that location of right whales (Daoust et al., 2018). Similarly, a small-stress ship strike could damage structures important for life functions (e.g. baleen) and therefore also produce a mortality. In the meantime, the present model permits a first-order simulation of strikes at various body parts through predictions of compression stress for given a strike, as a function of blubber and sublayer thickness. Thus, for example, our simulations reveal that compression stress

may exceed bone strength if the vessel strikes a region of the animal with thin blubber and sublayer cover, such as the head.

The simulations with the four-layer model reveal that the area of impact is another important factor, as was suspected from the scaling derived in the one-layer model. Determining this area is collision-specific, involving the profile of the vessel bow and the whale size and shape. The simulations in this study used relatively standard impact areas (see Appendix B), but the model takes the geometry of the impact zone as an adjustable parameter, which permits simulation of a wide range of collisions, from the fishing boats and container ships of the test cases shown here, to the case of low-mass, high-velocity oceanic racing vessels, which may present a serious hazard to whales because of the small impact area of their narrow keels and daggerboards (Ritter, 2012).

Although the models presented in this research incorporate some of the most important factors in estimating the reactive forces of a ship strike, there are other variables that ought to be considered in more advanced models. These include the angle of the collision, the articulation and architecture of the whale body (i.e., the separation of the body parts into separate but connected masses), whale behaviors such as evasion, and the possibility of skin lacerations caused by shearing forces exerted across small areas, such as may be caused by ship propellers (Campbell-Malone et al., 2008; Sharp et al., 2019; Wiley et al., 2016).

4.1 | Conclusions

We have shown that a four-layer dynamical model of ships striking whales produces results that are in good agreement with a more sophisticated finite-element model. This is important because the present model is so simple and efficient that it can be used within a GUI-based application (to be described separately) that can run simulations quickly enough to respond to a user's interactive explorations of the effects of altering relevant variables (e.g., vessel size and speed, whale size, and blubber thickness). The calibration of the model with observations of whale injuries from known strikes gives us the ability to identify critical speeds for vessels of any given mass, colliding with a whale of any given properties. This may prove beneficial in the context of species at risk of extinction such as the North Atlantic right whale, as these simulations offer guidance immediately, thus avoiding delays inherent in statistical prediction that must be based on the collection of data from prior collision events involving animals that are already at risk.

We used this tool to investigate the likely injuries incurred for two important classes of vessel that are of great concern to the conservation of North Atlantic right whales. The results suggest that (1) there is no reasonable transiting speed at which large vessels could strike a whale without a large risk of lethally injuring the animal, and that (2) vessels of all sizes pose a threat to seriously injure or kill whales.

The analysis for large vessels reveals that the speed limits commonly under discussion in the research and management communities (i.e., 10 knots) will provide only small reductions in the probability of lethal ship strikes. Thus, for large vessels, the only practical way of reducing the risk of lethal collisions is to reduce the co-occurrence of these vessels with whales. Mechanisms to do this include establishing exclusion areas for vessels (e.g., International Maritime Organization Areas to be Avoided), altering shipping lanes, and revising traffic separation schemes. Implementing these tools will require knowledge of where and when elevated probabilities for ship strikes exist. Work to provide this knowledge is currently being undertaken by numerous researchers (e.g., M. K. Carr, personal communication, July 2020).

By contrast, there may be more opportunities available for small vessels to mitigate their risk of causing a lethal ship strike. Owing to the proximity of the crew to the ocean surface on small vessels, along with the maneuverability and responsiveness of such craft (Schoeman et al., 2020; Wiley et al., 2016), collisions may be avoided by a combination of last-minute detection and evasive action. Therefore, for small vessels at least, there is a reason to hope that a combination of speed restrictions and having crew posted to watch for surfacing whales may be an effective way to reduce the incidence of whale injury and mortality.

ACKNOWLEDGMENTS

The work we present here benefitted from discussions with our Dalhousie University colleagues M. K. Carr and C. T. Taggart. In addition, we are grateful for the very detailed and helpful comments made by two anonymous reviewers.

AUTHOR CONTRIBUTIONS

Dan Kelley: Conceptualization; data curation; formal analysis; funding acquisition; investigation; methodology; project administration; software; supervision; visualization; writing-original draft; writing-review and editing. **James Vlasic:** Investigation; methodology; validation; writing-original draft. **Sean Brillant:** Conceptualization; funding acquisition; methodology; project administration; supervision; writing-original draft; writing-review and editing.

ORCID

Dan E. Kelley https://orcid.org/0000-0001-7808-5911
James P. Vlasic https://orcid.org/0000-0002-3846-4391
Sean W. Brillant https://orcid.org/0000-0001-5494-3475

REFERENCES

Campbell-Malone, R., Barco, S. G., Daoust, P.-Y., Knowlton, A. R., McLellan, W. A., Rotstein, D. S., & Moore, M. J. (2008). Gross and histologic evidence of sharp and blunt trauma in North Atlantic right whales (*Eubalaena glacialis*) killed by vessels. *Journal of Zoo and Wildlife Medicine*, *39*, 37–55.

Conn, P. B., & Silber, G. K. (2013). Vessel speed restrictions reduce risk of collision-related mortality for North Atlantic right whales. *Ecosphere*, *4*(4), 43.

Daoust, P.-Y., Couture, E. L., Wimmer, T., & Bourque, L. (2018). Incident report: North Atlantic right whale mortality event in the Gulf of St. Lawrence, 2017. Collaborative report produced by Canadian Wildlife Health Cooperative, Marine Animal Response Society, and Fisheries and Oceans Canada. http://1www.cwhc-rcsf.ca/docs/technical_reports/NARW_Incident_Report-%2020180405%20MD.pdf

Davies, K. T. A., & Brillant, S. W. (2019). Mass human-caused mortality spurs federal action to protect endangered North Atlantic right whales in Canada. *Marine Policy*, *104*, 157–162.

Fortune, S. M. E., Trites, A. W., Perryman, W. L., Moore, M. J., Pettis, H. M., & Lynn, M. S. (2012). Growth and rapid early development of North Atlantic right whales (*Eubalaena glacialis*). *Journal of Mammalogy*, *93*, 1342–1354.

Gende, S. M., Vose, L., Baken, J., Gabriele, C. M., Preston, R., & Hendrix, A. N. (2019). Active whale avoidance by large ships: Components and constraints of a complementary approach to reducing ship strike risk. *Frontiers in Marine Science*, *6*, 19.

Hatch, L., Clark, C., Merrick, R., Van Parijs, S., Ponirakis, D., Schwehr, K., … Wiley, D. (2008). Characterizing the relative contributions of large vessels to total ocean noise fields: A case study using the Gerry E. Studds Stellwagen Bank National Marine Sanctuary. *Environmental Management*, *42*, 735–752.

Jensen, A. S., & Silber, G. K. (2004). *Large whale ship strike database* (NOAA Technical Memorandum NMFS-OPR). Washington, DC: U.S. Department of Commerce.

Kite-Powell, H. L., Knowlton, A., & Brown, M. (2007). Modeling the effect of vessel speed on right whale ship strike risk. *Project report for NOAA/NMFS Project NA04NMF47202394* (Vol. 2).

Kraus, S. D., Brown, M. W., Caswell, H., Clark, C. W., Fujiwara, M., Hamilton, P. K., … Rolland, R. M. (2005). North Atlantic right whales in crisis. *Science*, *309*(5734), 561–562.

Laist, D. W., Knowlton, A. R., Mead, J. G., Collet, A. S., & Podesta, M. (2001). Collisions between ships and whales. *Marine Mammal Science*, *17*, 35–75.

Leighfield, T. (2003). Final large whale necropsy report Field Number: MJM03-01Eg, CCSN03-160Eg, New England Aquarium catalog ID # EG 2150. Charleston, SC.

MAN Diesel & Turbo. (2011). *Basic principles of propulsion*. Denmark: Frederikshavn.

Moore, M. J., van der Hoop, J., Barco, S. G., Costidis, A. M., Gulland, F. M., Jepson, P. D., … McLellan, W. A. (2013). Criteria and case definitions for serious injury and death of pinnipeds and cetaceans caused by anthropogenic trauma. *Diseases of Aquatic Organisms*, *103*, 229–264.

Neilson, J. L., Gabriele, C. M., Jensen, A. S., Jackson, K., & Straley, J. M. (2012). Summary of reported whale-vessel collisions in Alaskan waters. *Journal of Marine Biology*, *2012*, 18.

R Core Team. (2020). *R: A language and environment for statistical computing*. Vienna, Austria: R Foundation for Statistical Computing.

Raymond, J. J. (2007). *Development of a numerical model to predict impact forces on a North Atlantic right whale during collision with a vessel* (Master's thesis). University of New Hampshire, Durham, NH.

Ritter, F. (2012). Collisions of sailing vessels with cetaceans worldwide: First insights into a seemingly growing problem. *Journal of Cetacean Research and Management*, *12*, 119–127.

Schoeman, R. P., Patterson-Abrolat, C., & Plön, S. (2020). A global review of vessel collisions with marine animals. *Frontiers in Marine Science*, *7*(May), 1–25.

Sharp, S. M., McLellan, W. A., Rotstein, D. S., Costidis, A. M., Barco, S. G., Durham, K., … Moore, M. J. (2019). Gross and histopathologic diagnoses from North Atlantic right whale *Eubalaena glacialis* mortalities between 2003 and 2018. *Diseases of Aquatic Organisms*, *135*, 1–31.

Simard, Y., Roy, N., Giard, S., & Aulanier, F. (2019). North Atlantic right whale shift to the Gulf of St. Lawrence in 2015, revealed by long-term passive acoustics. *Endangered Species Research*, *40*, 271–284.

Soetaert, K., Petzoldt, T., & Setzer, R. W. (2010). Solving differential equations in R: Package deSolve. *Journal of Statistical Software*, *1*(9).

Soldevilla, M. S., McKenna, M. E., Wiggins, S. M., Shadwick, R. E., Cranford, T. W., & Hildebrand, J. A. (2005). Cuvier's beaked whale (*Ziphius cavirostris*) head tissues: Physical properties and CT imaging. *Journal of Experimental Biology*, *208*, 2319–2332.

Transport Canada. (2018). Protecting North Atlantic right whales from collisions with ships in the Gulf of St. Lawrence. Retrieved August 20, 2008, from https://www.tc.gc.ca/en/services/marine/navigation-marine-conditions/protecting-north-atlantic-right-whales-collisions-ships-gulf-st-lawrence.html

U.S. Federal Register (2008). Endangered Fish and Wildlife; Final Rule to Implement Speed Restrictions to Reduce the Threat of Ship Collisions with North Atlantic Right Whales. FR 73(198):60173–60191 (7 October 2008). Washington, DC: National Marine Fisheries Service, National Oceanic and Atmospheric Administration, Department of Commerce.

van der Hoop, J. M., Moore, M. J., Barco, S. G., Cole, T. V. N., Daoust, P.-Y., Henry, A. G., … Solow, A. R. (2013). Assessment of management to mitigate anthropogenic effects on large whales. *Conservation Biology*, *27*, 121–131.

van der Hoop, J. M., Vanderlaan, A. S. M., & Taggart, C. T. (2012). Absolute probability estimates of lethal vessel strikes to North Atlantic right whales in Roseway Basin, Scotian Shelf. *Ecological Applications*, *22*, 2021–2033.

van Manen, J. D., & van Oossanen, P. (1988). Resistance. In E. V. Lewis (Ed.), *Principles of naval architecture (Second Revision), Volume II • Resistance, propulsion and vibration* (2nd ed.). Jersey City, NJ: Society of Naval Architects and Marine Engineers.

Vanderlaan, A. S. M., & Taggart, C. T. (2007). Vessel collisions with whales: The probability of lethal injury based on vessel speed. *Marine Mammal Science*, *23*, 144–156.

Vanderlaan, A. S. M., & Taggart, C. T. (2009). Efficacy of a voluntary area to be avoided to reduce risk of lethal vessel strikes to endangered whales. *Conservation Biology*, *23*, 1467–1474.

Vanderlaan, A. S. M., Taggart, C. T., Serdynska, A., Kenney, R. D., & Brown, M. W. (2008). Reducing the risk of lethal encounters: Vessels and right whales in the Bay of Fundy and on the Scotian Shelf. *Endangered Species Research*, *4*, 283–297.

Wiley, D. N., Mayo, C. A., Maloney, E. M., & Moore, M. J. (2016). Vessel strike mitigation lessons from direct observations involving two collisions between noncommercial vessels and North Atlantic right whales (*Eubalaena glacialis*). *Marine Mammal Science*, *32*, 1501–1509.

Wiley, D. N., Thompson, M., Pace, R. M., & Levenson, J. (2011). Modeling speed restrictions to mitigate lethal collisions between ships and whales in the Stellwagen Bank National Marine Sanctuary, USA. *Biological Conservation*, *144*, 2377–2381.

Woods Hole Oceanographic Institution. (1952). *Marine fouling and its prevention* (prepared for Bureau of Ships, Navy Department). Annapolis, MD: United States Naval Institute.

SUPPORTING INFORMATION

Additional supporting information may be found online in the Supporting Information section at the end of this article.

How to cite this article: Kelley DE, Vlasic JP, Brillant SW. Assessing the lethality of ship strikes on whales using simple biophysical models. *Mar Mam Sci*. 2020;1–17. https://doi.org/10.1111/mms.12745